

## Angle-resolved photoemission study of the (100) surface of a $\text{ZrN}_{0.93}$ single crystal

J. Lindström, L. I. Johansson, and A. Callenås

*Department of Physics and Measurement Technology, Linköping University, S-581 83 Linköping, Sweden*

D. S. L. Law

*Science and Engineering Research Council, Daresbury Laboratory, Daresbury Warrington WA4 4AD, United Kingdom*

A. N. Christensen

*Department of Chemistry, Aarhus University, DK-8000 Aarhus C, Denmark*

(Received 4 December 1986)

The (100) surface of a  $\text{ZrN}_{0.93}$  single crystal has been studied using angle-resolved photoemission and synchrotron radiation. A mapping of the bulk-band structure is presented and compared with an augmented-plane-wave band structure, calculated for stoichiometric composition. The experimentally determined bands are found to be located deeper below the Fermi energy than the calculated bands but the dispersions agree fairly well. A surface state is observed at 3.8 eV binding energy, for photon energies below 24 eV, and a structure interpreted as arising from vacancy induced states is observed at a binding energy of 2.1 eV for photon energies above 30 eV. The latter structure is found to exhibit a strong intensity modulation with photon energy. This intensity modulation is compared with the resonance enhancement observed in the emission from states just below the Fermi energy above the Zr 4*p* absorption threshold.

### INTRODUCTION

Zirconium nitride,  $\text{ZrN}$ , exhibits many interesting physical and electrical properties<sup>1</sup> characteristic of the refractory transition-metal carbides and nitrides (TMCN). It has a high melting point (2982°C) and hardness, which has led to its use as coatings to increase the wear resistance, for instance on cutting tools. All the TMCN are metallic with a high electrical conductivity, and some are very good superconductors with transition temperatures of about 18 K. It is known that these materials rarely exist in the stoichiometric composition, but contain vacancies mostly on the nonmetal sites in the lattice. The vacancies are very important for the properties of TMCN, such as hardness, specific heat, electrical conductivity, and superconductivity. The physical properties of all these materials are closely related to their electronic structure. Therefore detailed experimental investigations of the electronic structure of these materials using the angle-resolved photoemission technique seem well motivated.

The photoemission studies of  $\text{ZrN}$  reported previously have been made either angle-integrated<sup>2-5</sup> on polycrystalline samples or angle-resolved using conventional light sources.<sup>6,7</sup> In the present study we have utilized synchrotron radiation, in the energy range 17–58 eV, and a single-crystal sample  $\text{ZrN}_{0.93}(100)$ . Our angle-resolved measurements allow a mapping of the bulk-band structure to be made along the high-symmetry  $\Gamma$ –*X* direction by using the direct transition model and the band structure of  $\text{ZrN}_{1.0}$  calculated<sup>8</sup> using the augmented-plane-wave (APW) method. A comparison between experimental and theoretical results is made. Most of the structures observed in the photoemission spectra can be interpreted as arising from direct bulk-band transitions, but there are

some features that cannot be explained by the calculated band structure of stoichiometric  $\text{ZrN}$ . A surface state is observed at 3.8 eV binding energy in the spectra recorded at photon energies below 24 eV. This surface state has been identified in earlier angle-resolved studies employing resonance radiation,<sup>6,7</sup> but not in the angle-integrated studies.<sup>2-5</sup> In some of the latter studies made on polycrystalline substoichiometric samples<sup>2,3</sup> a structure was observed around 2-eV binding energy and was interpreted as arising from vacancy-induced states. It was claimed in these investigations that such a structure was not expected to be observed on samples that had been cleaned *in situ* by flash heatings since that would produce a surface layer of stoichiometric composition. We have performed our experiments on a crystal with a bulk chemical composition of  $\text{ZrN}_{0.93}$ , which was cleaned *in situ* by repeated flash heatings. In the spectra recorded at photon energies above 30 eV we do indeed observe a structure at 2.1-eV binding energy that we interpret as due to vacancy-induced states. This interpretation is firmly supported by the results obtained in a very recent theoretical work.<sup>9</sup>

The photon absorption coefficient, as reflected by a constant-final-state spectrum, shows a strong resonance behavior above the Zr 4*p* threshold. This complicates the interpretation of the recorded spectra since contribution from super Coster-Kronig decays following the 4*p*-4*d* photon absorption may become significant. A strong resonance behavior is actually observed in the emission from states just below the Fermi energy at photon energies between about 35 and 45 eV. The peak interpreted as originating from vacancy states is also found to exhibit intensity modulations with photon energy, contrary to previous experimental findings on  $\text{ZrN}$ .<sup>2</sup> At photon energies above about 45 eV our experimental spectra are found to be dominated by density of states features.

## EXPERIMENTAL

Synchrotron radiation from beam line 6.2 at Daresbury Laboratory was utilized for carrying out angle-resolved photoemission measurements on ZrN(100). This beam line is equipped with a toroidal grating monochromator and an angle-resolved ADES 400 electron spectrometer, operating at a base pressure of less than  $2 \times 10^{-10}$  torr. The photon energy resolution of the monochromator and the energy resolution of the analyzer, respectively, were both selected to be  $< 0.2$  eV, giving an overall energy resolution of  $< 0.3$  eV. The acceptance angle of the electron analyzer was  $\pm 2^\circ$ .

The ZrN single-crystal used, which had been grown by a zone-annealing technique,<sup>10,6</sup> crystallizes in the NaCl structure. The crystal was cleaned *in situ* by repeated flash heatings to about 1300°C. This cleaning procedure has been found to produce a clean and well-ordered (100) surface, as checked by low-energy electron diffraction and Auger electron spectroscopy. The bulk chemical composition of the crystal has been determined to be ZrN<sub>0.93</sub>, and it thus contains a few percent vacancies in the nitrogen lattice. The cleaning procedure, flash heatings, is not expected to give rise to any significant compositional changes in the surface region,<sup>11,12</sup> although this possibility has been proposed by some authors.<sup>2,3,13</sup> This point is further discussed below in connection with an observed vacancy-induced state. In all spectra presented below the energy is referenced to the Fermi energy. The angle of incidence  $\theta_i$  of the linearly polarized radiation and the electron emission angle  $\theta_e$  are given relative to the surface normal of the sample.

## RESULTS AND DISCUSSION

A wide scan spectrum of ZrN recorded at a photon energy of 56 eV is shown in Fig. 1. A valence-band structure arising from hybridized Zr 4*d* and N 2*p* states distri-

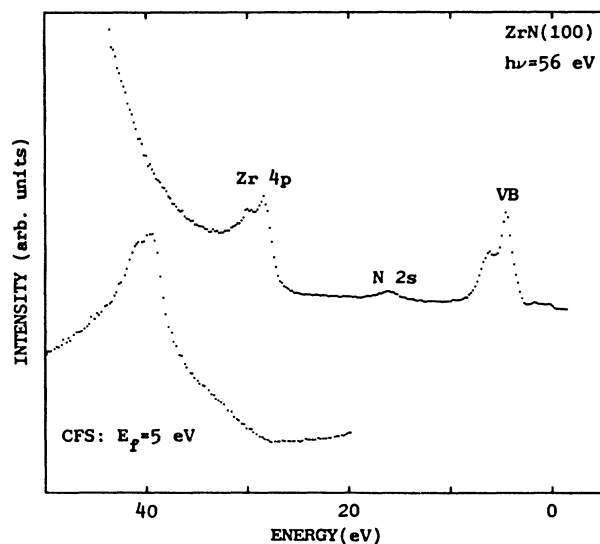
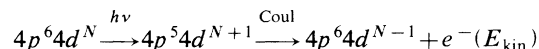


FIG. 1. Normal emission angle-resolved spectrum, at 56-eV photon energy and  $\theta_i = 30^\circ$ , of ZrN<sub>0.93</sub>(100). The inserted CFS spectrum was recorded at a final-state energy of  $E_f = 5$  eV.

buted between about 0 and 8 eV, a N 2*s* peak around 17 eV, and a Zr 4*p* doublet structure around 29 eV are clearly discernable in the spectrum. Inserted in the figure is a CFS (constant-final-state) spectrum mimicking the absorption coefficient and showing the absorption resonance above the Zr 4*p* threshold. The maximum of the resonance is approximately 10 eV above the Zr 4*p* absorption threshold. The presence of this absorption resonance introduces complications in the interpretation of the angle-resolved spectra recorded at photon energies above about 30 eV. Resonance photoemission processes like



may occur and give rise to spectral features interfering with the contribution from direct bulk-band transitions. Such resonance features are not expected to exhibit any appreciable dispersion with photon energy but merely intensity modulations. Therefore it should be possible to separate out such features from structures arising from direct interband transitions since the latter are expected to show the dispersion predicted by the calculated band structure.

Angle-resolved photoemission spectra from ZrN(100) recorded at normal electron emission using three different photon energies, 16.8, 21, and 36 eV, and two different incident angles of the radiation are shown in Fig. 2. The 16.8-eV spectra were recorded using a resonance lamp in another ADES 400 spectrometer. A number of structures are clearly resolved in the spectra and are labeled from *A* to *F* in the figure. The main symmetry character of the initial states from which these structures originate can be determined from the dependence of their relative intensity on the angle of incidence,  $\theta_i$ . At normal electron emission, symmetry selection rules<sup>14</sup> show that the radiation component parallel to the surface can give rise to emission only from initial states of  $\Delta_5$  symmetry and the component perpendicular to the surface only from initial states of  $\Delta_1$  symmetry. This means that the relative intensity ratio between  $\Delta_5$  and  $\Delta_1$  peaks in a spectrum will decrease with increasing  $\theta_i$ . The observed variation in relative peak intensity with angle of incidence, illustrated in Fig. 2, clearly indicates that peaks *B* and *C* originate from initial states of  $\Delta_5$  symmetry while peaks *A* and *D* originate from initial states of  $\Delta_1$  character. Peaks *E* and *F* do not exhibit any pronounced polarization dependence in these spectra. Internal limitations in the electron spectrometer prevented a decrease of  $\theta_i$  below thirty degrees; otherwise bigger relative differences between  $\Delta_5$  and  $\Delta_1$  derived peaks would have been observed. These symmetry assignments for peaks *A*, *B*, and *C* agree, however, with earlier experimental results.<sup>6</sup>

Normal electron emission spectra recorded at  $\theta_i = 30^\circ$  using photon energies between 17 and 44 eV are shown in Figs. 3 and 4. Dispersion with photon energy is clearly observed for peaks *A* and *B*, and it can therefore be concluded that they arise from direct bulk-band transitions. Peak *C* shows no dispersion, and it is only resolved at photon energies below 24 eV. It has earlier been interpreted as originating from a Tamm surface state<sup>6,7</sup> pulled off the  $\Delta_5$  bulk band by the change in electrostatic potential at the surface. New theoretical calculations,<sup>15</sup> however,

indicate that a surface state can also arise from a vacancy gradient in the surface layers. Structures *D–G* appear most clearly in the spectra recorded at higher photon energies, but they show no appreciable dispersion with photon energy. The spectra shown in Figs. 3 and 4 allow a mapping of the band structure along the  $\Gamma$ – $X$  direction to be made utilizing the theoretical band structure of  $\text{ZrN}_{1.0}$ , calculated using the linearized augmented-plane-wave (LAPW) method.<sup>6,8</sup> Direct transitions are assumed and that only  $\Delta_1$  final-state bands contribute at normal electron emission. For photon energies between 17 and 27 eV the calculated  $\Delta_1$  final-state bands were used when mapping the initial-state bands dispersions. Above 27 eV, however, a free-electron band was used as the final-state band instead. The reason for this is illustrated in Fig. 5, where the theoretical final-state  $\Delta_1$  bands and the fitted

free-electron band are shown. Band gaps and two relatively flat final-state bands appear in the calculated final-state band structure, at about 30 eV which complicates the band mapping. When experimental and calculated band structures are compared, the distinctions between them have to be remembered. Photoemission probes excitations which include electron and hole lifetimes and correlation effects, while band-structure calculations describe ground-state properties and are based on one-electron descriptions.

Our experimental results along the  $\Gamma$ – $X$  direction are shown in Fig. 6 together with the calculated band structure. Solid circles represent the experimentally determined energy locations of the  $\Delta_1$  and  $\Delta_5$  bulk bands and of the surface state with  $\Delta_5$  symmetry. The triangles represent the location of peak *D*, and the open circles the energy positions of the structures *E–G*. The calculated  $\Delta_1$  and  $\Delta_5$  bulk bands are seen to reproduce the disper-

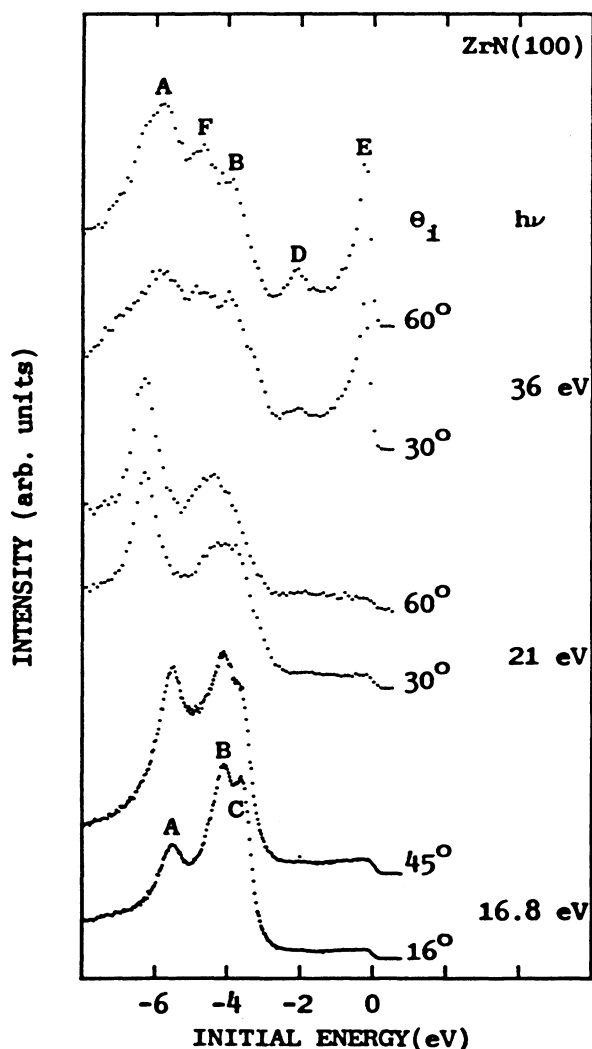


FIG. 2. Normal emission angle-resolved EDC's from  $\text{ZrN}_{0.93}(100)$  recorded at 16.8, 21, and 36 eV, and two different incident angles for each energy. The polarization dependence of peaks *A* and *D* indicate  $\Delta_1$  symmetry, while *B* and *C* indicate  $\Delta_5$  symmetry.

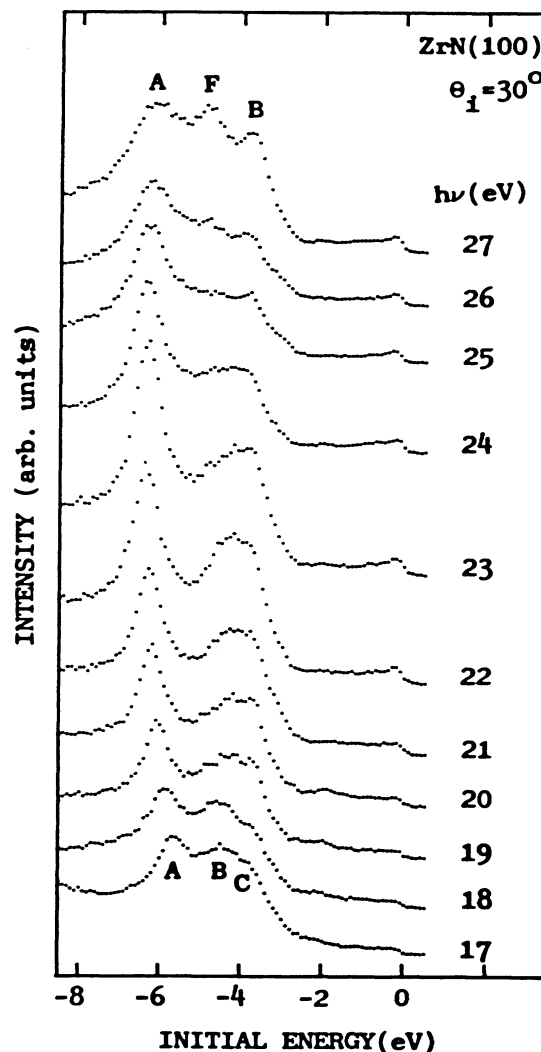


FIG. 3. Normal emission angle-resolved EDC's from  $\text{ZrN}_{0.93}(100)$ , recorded at  $\theta_i = 30^\circ$  for photon energies between 17 and 27 eV.

sions of the experimental bands (solid circles) fairly well, although the experimental results locate the bands deeper below the Fermi level. The  $\Delta_5$  band is at the  $\Gamma_{15}$  point about 1.3 eV below the corresponding calculated band, and the minimum of the  $\Delta_1$  band is about 0.4 eV below. The larger discrepancy in the position of the  $\Delta_5$  initial-state band could partly be a consequence of vacancy interactions affecting the  $\Delta_5$  states more strongly than the  $\Delta_1$  states.<sup>9</sup> Calculations<sup>9</sup> indicate that the  $\Delta_5$  states are shifted somewhat closer to  $E_F$  in crystals of stoichiometric composition. The difference observed, 1.3 eV, is, however, much too large to be explained by this effect only. The determined dispersion of the  $\Delta_1$  band is uncertain close to  $\Gamma$ , but it is clear that the experimentally determined width of the  $\Delta_1$  band is smaller than the calculated band width. This uncertainty is possibly due to the fact that the initial-state band is steep and has a large slope in this region almost parallel to the final-state band,

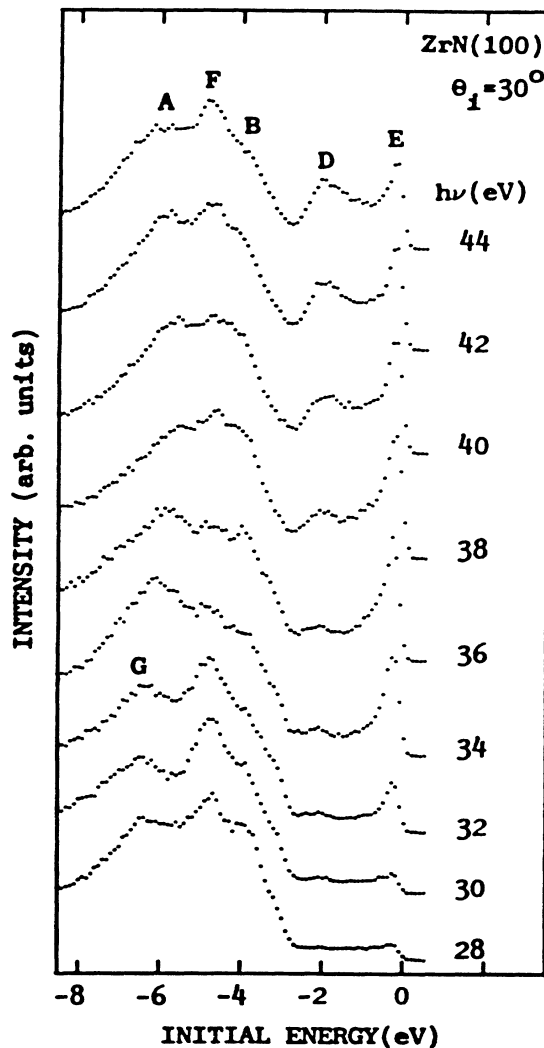


FIG. 4. Normal emission angle-resolved EDC's from  $ZrN_{0.93}(100)$ , recorded at  $\theta_i = 30^\circ$  for photon energies between 28 and 44 eV.

therefore giving an appreciable contribution to the peak width.<sup>16</sup> The greater peak width makes it difficult to follow the dispersion. If one, however, assumes that the experimental  $\Gamma_{15}$  point is the top of the  $\Delta_1$  band, then the determined  $\Delta_1$  bandwidth is approximately 26% smaller than calculated. The surface state, split off from the bulk  $\Delta_5$  band, is found to merge with the bulk  $\Delta_5$  contribution at photon energies above 24 eV, i.e., when approaching  $\Gamma$ . Similar observations about the location and dispersion of experimentally determined bulk bands and a surface state have been made earlier in experiments on a substoichiometric TiN(100) crystal.<sup>17</sup>

The triangles around  $-2.1$  eV in Fig. 6 represent the location of peak *D*, which appears in the spectra recorded at photon energies above 30 eV, see Figs. 2–4. This structure cannot originate from the  $\Delta_2$  initial-state band since it shows no dispersion and has a polarization dependence characteristic for states of  $\Delta_1$  symmetry, see Fig. 2. At normal electron emission transitions from the  $\Delta_2$  initial-state band are, moreover, forbidden by symmetry selection rules. A structure located around  $-2$  eV has been observed in earlier angle-integrated studies<sup>2–4</sup> on substoichiometric polycrystalline samples of ZrN and TiN and been interpreted as originating from vacancy-induced

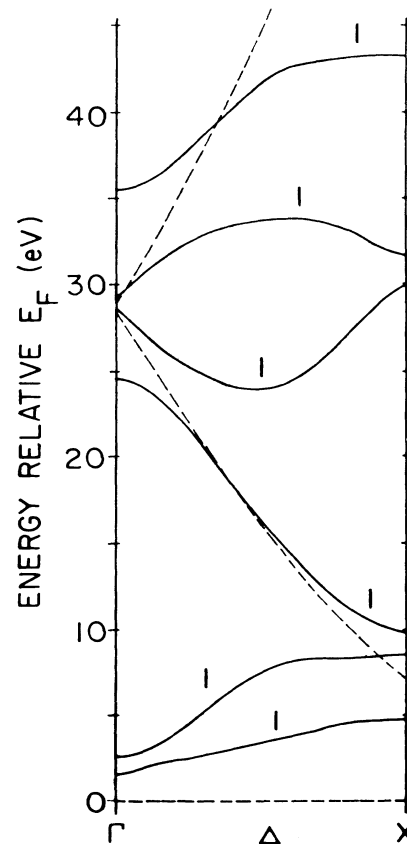


FIG. 5. The calculated APW  $\Delta_1$  final-state band structure (—) and a fitted free-electron band (---). In mapping the band structure both the calculated ( $\leq 27$  eV) and the free-electron ( $> 27$  eV) bands have been used.

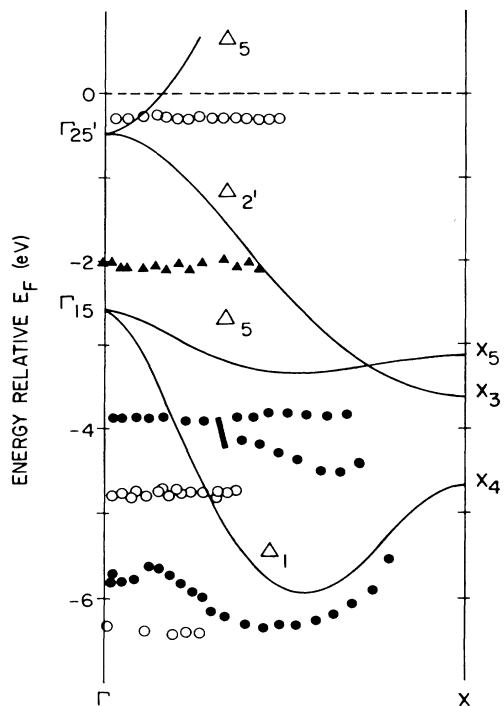


FIG. 6. Comparison between experimental and calculated initial state band structure. The solid circles (●) represent peaks interpreted as originating from the  $\Delta_1$  and  $\Delta_5$  initial states, triangles (▲) from vacancy-induced states, and the open circles (○) are DOS effects.

states. Theoretical calculations showing how vacancies affect the electronic structure of nitrides were recently published.<sup>9,13,15,18-20</sup> These results show<sup>9</sup> for non-stoichiometric ZrN that a vacancy-induced structure appears around  $-2$  eV in spectra calculated at photon energies larger than about 30 eV. These theoretical and experimental findings suggest that the observed structure around  $-2.1$  eV in our ZrN spectra most probably originates from vacancy-induced states.

Peak *E* at the Fermi energy and also the vacancy-induced peak *D* show a resonance behavior in the spectra, which seems to be related to  $4p-4d$  transitions. In order to visualize the resonance effects more clearly, the ratios of the areas under the vacancy-induced peak (*D*) and the peak at the Fermi energy (*E*), respectively, and the area under the valence-band peaks (between  $-2.7$  and  $-8.5$  eV), were calculated. The photon energy dependence of these ratios is shown in Fig. 7. Both the onset at approximately 30 eV and the maximum around 38 eV for peak *E*, coincide well with the CFS spectrum. This indicates that the initial states at the Fermi energy are mainly of *d* character, in agreement with the partial density of states results.<sup>19</sup> The vacancy-induced peak has a weak resonance maximum around 44 eV, and the onset is roughly at 36 eV. This resonance is thus delayed about 6 eV compared with the resonance for the peak at the Fermi energy. In an earlier angle-integrated study of ZrN (Ref. 2) no resonance behavior of the vacancy peak was found. This was

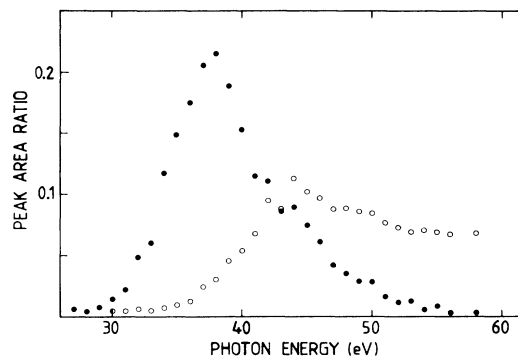


FIG. 7. The ratios of the peak area below the vacancy state, peak *D*, (○), respectively, the peak *E* at the Fermi energy (●) and the area below the valence-band peaks, between  $-2.7$  and  $-8.5$  eV.

taken as evidence that the vacancy states have little *d* character. Our results show, however, that the peak has a resonance behavior and consequently that the states may well have an appreciable extent of *d* character, as suggested by theoretical work on vacancies in ZrN,<sup>9</sup> TiN,<sup>18</sup> and NbC.<sup>21,22</sup>

It has been argued by some authors that the cleaning technique we use, flash heatings, probably gives a stoichiometric surface layer.<sup>2,3,13</sup> No experimental evidence of such an effect has, however, been reported to our knowledge. On the contrary results reported<sup>11,12</sup> from angle-resolved x-ray photoemission and ion scattering experiments on TiC(100) show that no concentration gradient is detected after flash heatings to about 1500°C. If a high concentration of vacancies was created in the surface layer deliberately by ion sputtering, however, the vacancy concentration was shown<sup>23</sup> to be reduced by flash heatings, but it was not stated that a stoichiometric surface layer was created. Our observation of the vacancy-induced state indicates that vacancies do exist in the surface region, i.e., in the outermost atomic layers, also after repeated flash-heating cycles. If a composition close to the bulk composition persists in the surface region it is not surprising that a vacancy-induced structure is observed since the measurements were made on a sub-stoichiometric sample ZrN<sub>0.93</sub>. We can, however, not rule out the possibility that a small composition gradient may arise at the surface. Thus whether the observed surface state, peak *C* in the discussion above, originates from a potential shift in the top layer or from a small composition gradient in the topmost layers cannot be determined from these experiments.

The open circles in Fig. 6 represent the positions of the structures *E*, *F*, and *G* which are most pronounced at high photon energies, see Figs. 2-4. These structures seem to be density of states (DOS) features since they do not show any dispersion and no pronounced polarization dependence. They appear at photon energies where resonance photoemission effects make a significant contribution to the intensity of emitted electrons. Direct transitions from the uppermost  $\Delta_5$  initial-state band should appear only at photon energies between 24 and 36 eV, ac-

cording to the calculated band structure. Peak *E* appears most strongly at too high photon energies to be explained solely by direct bulk-band transitions. That the photoemission spectra reflect more of the total DOS when increasing the photon energy is clearly illustrated in Fig. 8 where spectra recorded at 45 and 58 eV are shown together with a DOS spectrum calculated<sup>8</sup> for ZrN<sub>1.0</sub>. The resemblance between the experimental and theoretical spectra is good, apart from the vacancy-induced structure around -2 eV in the experimental spectra which naturally is not present in the DOS spectrum of stoichiometric ZrN. The most pronounced peaks in the experimental spectra and the calculated DOS spectrum coincides very well, and it is quite evident that DOS effects dominate the spectra at these high photon energies. This is, however, not unexpected since a larger number of usable final states become available when the photon energy is increased. Due to the finite acceptance angle of the electron analyzer, a larger part of the Brillouin zone is probed when increasing the photon energy. Disorder, thermal or

compositional, destroys *k* conservation and can give contributions to the DOS.<sup>24,25</sup> The phonon-aided indirect processes also become more important as the kinetic energies of the photoelectrons increases. Defects like vacancies and surface roughness are expected to weaken the *k* conservation<sup>25</sup> and contribute to the DOS. Surface roughness could also lead to a broadening of the peak widths via diffuse scattering at the surface.

## SUMMARY

The bulk and surface electronic structure of a ZrN<sub>0.93</sub> single crystal was measured by utilizing angle-resolved photoemission. The experiment was carried out on the (100) surface. Bulk initial states of  $\Delta_1$  and  $\Delta_5$  symmetry were identified by their polarization dependence. A mapping of the initial-state band dispersions and locations was made using the calculated  $\Delta_1$  final-state bands and a fitted free-electron band. The dispersions determined for the  $\Delta_1$  and  $\Delta_5$  initial-state bands were compared with a LAPW calculation made for stoichiometric composition of the crystal. The theoretical dispersions were found to agree fairly well with the experimental results, but discrepancies in band locations were observed. The experimentally determined bands were found to be located considerably deeper below the Fermi energy than the corresponding calculated bands, and the  $\Delta_1$  band width was approximately 26% smaller than calculated.

A surface state of  $\Delta_5$  symmetry was observed at a binding energy of 3.8 eV in agreement with earlier results.<sup>6,7</sup> A vacancy induced peak, which showed no dispersion, was observed at 2.1-eV binding energy. It appeared in the spectra at photon energies above 30 eV, which explains why it was not observed in an earlier angle-resolved study,<sup>6</sup> where He I and Ne I radiation was used. The polarization dependence indicates that it has " $\Delta_1$ -like" symmetry. This vacancy-induced peak showed, contrary to previous experimental observations, a resonance behavior above the Zr 4*p* absorption threshold. This indicates that the vacancy states may have *d* character to a certain extent, which recent theoretical results also suggest.<sup>9</sup> The fact that we see this vacancy peak in the spectra so clearly indicates that our cleaning technique, flash heatings, do not produce a stoichiometric surface as has been proposed.

A peak at the Fermi energy also showed a strong resonance behavior which, in accordance with partial DOS results, indicates that it originates mainly from *d*-like states. At high photon energies DOS features begin to show up in the spectra. For energies above 44 eV they completely dominate the spectra as illustrated by a comparison with a calculated DOS spectrum.

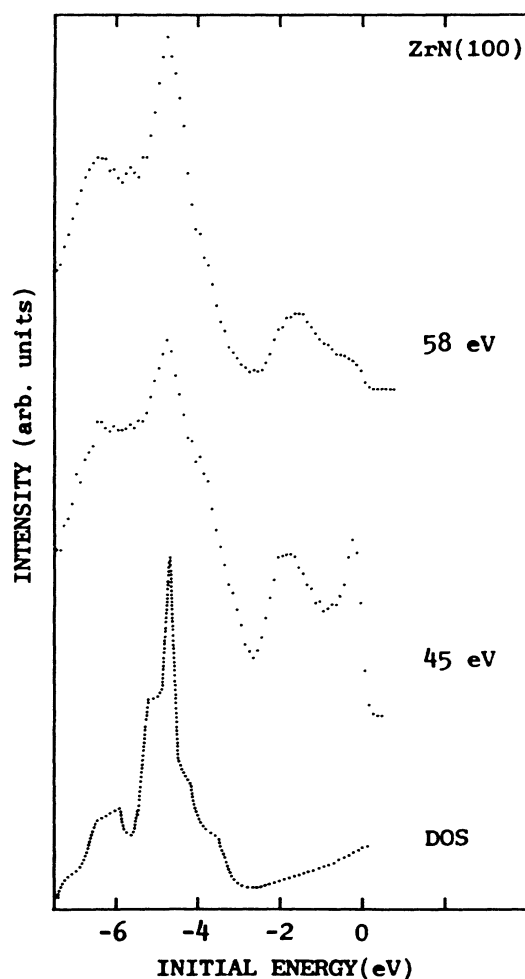


FIG. 8. Comparison between normal emission angle-resolved spectra recorded at 45 and 58 eV photon energy and a calculated (Refs. 6 and 8) DOS spectrum for stoichiometric ZrN.

## ACKNOWLEDGMENTS

The authors want to thank the staff at the Daresbury Laboratory for their assistance during the experiments. The financial support from the Swedish Natural Science Research Council, is gratefully acknowledged.

- <sup>1</sup>L. E. Toth, *Transition Metal Carbides and Nitrides* (Academic, New York, 1971).
- <sup>2</sup>R. D. Bringans and H. Höchst, *Phys. Rev. B* **30**, 5416 (1984).
- <sup>3</sup>H. Höchst, R. D. Bringans, P. Steiner, and Th. Wolf, *Phys. Rev. B* **25**, 7183 (1982).
- <sup>4</sup>L. Porte, *Solid State Commun.* **50**, 303 (1984).
- <sup>5</sup>W. K. Schubert, R. N. Shelton, and E. L. Wolf, *Phys. Rev. B* **24**, 6279 (1981).
- <sup>6</sup>A. Callenäs, L. I. Johansson, A. N. Christensen, K. Schwarz, P. Blaha, and J. Redinger, *Phys. Rev. B* **30**, 635 (1984).
- <sup>7</sup>A. Callenäs and L. I. Johansson, *Solid State Commun.* **52**, 143 (1984).
- <sup>8</sup>K. Schwarz, H. Ripplinger, and A. Neckel, *Z. Phys. B* **48**, 79 (1982).
- <sup>9</sup>J. Redinger, *Solid State Commun.* **61**, 133 (1987).
- <sup>10</sup>A. N. Christensen, *J. Cryst. Growth* **33**, 99 (1976).
- <sup>11</sup>C. Oshima, M. Aono, T. Tanaka, and S. Kawai, *Surf. Sci.* **102**, 312 (1981).
- <sup>12</sup>C. Oshima, M. Aono, S. Zaima, Y. Shibata, and S. Kawai, *J. Less-Common Met.* **82**, 69 (1981).
- <sup>13</sup>J. Redinger, P. Weinberger, and A. Neckel, *Phys. Rev. B* **35**, 5647 (1987).
- <sup>14</sup>J. Hermanson, *Solid State Commun.* **22**, 9 (1977).
- <sup>15</sup>J. Redinger and P. Weinberger, *Phys. Rev. B* **35**, 5652 (1987).
- <sup>16</sup>J. B. Pendry, in *Photoemission and the Electronic Properties of Surfaces*, edited by B. Feuerbacher, B. Fitton, and R. F. Willis (Wiley, New York, 1978), p. 94.
- <sup>17</sup>L. I. Johansson, A. Callenäs, P. M. Stefan, A. N. Christensen, and K. Schwarz, *Phys. Rev. B* **24**, 1883 (1981).
- <sup>18</sup>P. Marksteiner, P. Weinberger, A. Neckel, R. Zeller, and P. H. Dederichs, *Phys. Rev. B* **33**, 812 (1986).
- <sup>19</sup>J. Redinger, P. Marksteiner, and P. Weinberger (unpublished).
- <sup>20</sup>G. Schadler, P. Weinberger, A. Gonis, and J. Klima, *J. Phys. F* **15**, 1675 (1985).
- <sup>21</sup>G. Ries and H. Winter, *J. Phys. F* **10**, 1 (1980).
- <sup>22</sup>W. E. Pickett, B. M. Klein, and R. Zeller, *Phys. Rev. B* **34**, 2517 (1986).
- <sup>23</sup>M. Aono, Y. Hou, R. Souda, C. Oshima, S. Otani, and Y. Ishizawa, *Phys. Rev. Lett.* **50**, 1293 (1983).
- <sup>24</sup>N. J. Shevchik, *J. Phys. C* **10**, L555 (1977).
- <sup>25</sup>N. J. Shevchik, *Phys. Rev. B* **16**, 3428 (1977).